Developmental Status of the Multi-dimensional RELAP5

Lee, Sang-Yong, Choi, Chul-Jin

Korea Power Engineering Co.   150, Dukjin-Dong Yousung-Ku Daejeon, Korea

Abstract

Addition of the cross convective momentum terms can transform the RELAP5 into a multi-dimensional thermal-hydraulic code. The modified version has the convective momentum terms in cylindrical and spherical coordinate. It also has the viscous terms as well. But the friction in the cross flow junction is inserted for the consistency with the axial junction. The gravitational acceleration term is also updated for the individual coordinate system. Those modifications are implemented by using the pipe/multiple junction components and some connectivity data. Necessary data are produced by 'Input Generator', according to the user instruction. As a sample test case, a vessel with the direct vessel injection is investigated. Research area that needs further study is identified.

1. Introduction

Direct Vessel Injection (DVI) problem requires multi-dimensional code. RELAP5/MOD3.1[1] may be applied to model the multi-dimensional flow at downcomer by using multiple pipes and cross flow junctions. But the calculation results show many problems such as, vapor channeling at upper downcomer, persistent reverse flow in neighboring channels, extremely large circulation flow, and local circulation of flow at lower downcomer. A close investigation leads us to find the main source of the

troubles. Since no friction term is present in the MOD3.1 version, vapor channeling at upper downcomer

is inevitable if no compensatory form loss factor is introduced instead. The other problems are mainly

caused by the absence of the cross momentum flux terms. In this paper, appropriate corrections are made

and tested to mitigate or eliminate these problems. Also, the adoption of the spherical coordinate, which

is judged to be necessary for the lower plenum, requires the gravitational acceleration term for both the

polar and the radial direction.

Section 2 describes the theoretical aspects of this work. Section 3 explains the structure of input

generator. In section 4, results of the test application are discussed. One can find the items that need to be

studied further in the last section.

2. Description of Implementaion

The field equations for the momentum transport are written as follows.

In cylindrical coordinate:

$$
\frac{\partial v_r}{\partial t} + v_r \frac{\partial v_r}{\partial r} + \frac{v_\phi}{r} \frac{\partial v_r}{\partial \phi} + v_z \frac{\partial v_r}{\partial z} - \frac{v_\phi^2}{r} =
$$

$$
* \overline{}
$$

$$
- \frac{1}{\rho} \frac{\partial p}{\partial r} + g_r + \nu (\nabla^2 v_r - \frac{v_r}{r^2} - \frac{2}{r^2} \frac{\partial v_\phi}{\partial \phi})
$$

(2.1)

$$
\frac{\partial v_\phi}{\partial t} + v_r \frac{\partial v_\phi}{\partial r} + \frac{v_\phi}{r} \frac{\partial v_\phi}{\partial \phi} + v_z \frac{\partial v_\phi}{\partial z} + \frac{v_r v_\phi}{r} =
$$

$$
* \overline{}
$$

$$
- \frac{1}{\rho r} \frac{\partial p}{\partial r} + g_\phi + \nu (\nabla^2 v_\phi - \frac{v_\phi}{r^2} + \frac{2}{r^2} \frac{\partial v_r}{\partial \phi})
$$

(2.2)

$$
\frac{\partial v_z}{\partial t} + v_r \frac{\partial v_z}{\partial r} + \frac{v_\phi}{r} \frac{\partial v_z}{\partial \phi} + v_z \frac{\partial v_z}{\partial z} =
$$

$$
- \frac{1}{\rho} \frac{\partial p}{\partial z} + g_z + \nu \nabla^2 v_z
$$

(2.3)

2

In spherical coordinate:

$$\frac{\partial v_r}{\partial t} + v_r \frac{\partial v_r}{\partial r} + \frac{v_\phi}{r\sin\theta}\frac{\partial v_r}{\partial \phi} + \frac{v_\theta}{r}\frac{\partial v_r}{\partial \theta} - \underbrace{(\frac{v_\theta^2}{r} + \frac{v_\phi^2}{r})}_{*} =$$

$$-\frac{1}{\rho}\frac{\partial p}{\partial r} + g_r + \nu(\nabla^2 v_r - .....)$$

(2.4)

$$\frac{\partial v_\phi}{\partial t} + v_r \frac{\partial v_\phi}{\partial r} + \frac{v_\phi}{r\sin\theta}\frac{\partial v_\phi}{\partial \phi} + \frac{v_\theta}{r}\frac{\partial v_\phi}{\partial \theta} + \underbrace{(\frac{v_r v_\phi}{r} + \frac{v_\theta v_\phi \cot\theta}{r})}_{*} =$$

$$-\frac{1}{\rho r\sin\theta}\frac{\partial p}{\partial \phi} + g_\phi + \nu(\nabla^2 v_\phi - .....)$$

(2.5)

$$\frac{\partial v_\theta}{\partial t} + v_r \frac{\partial v_\theta}{\partial r} + \frac{v_\phi}{r\sin\theta}\frac{\partial v_\theta}{\partial \phi} + \frac{v_\theta}{r}\frac{\partial v_\theta}{\partial \theta} + \underbrace{(\frac{v_r v_\theta}{r} - \frac{v_\phi^2 \cot\theta}{r})}_{*} =$$

$$-\frac{1}{\rho r}\frac{\partial p}{\partial \theta} + g_\theta + \nu(\nabla^2 v_\theta - .....)$$

(2.6)

The length increment in each direction can be written, Δr, $r\Delta\phi$, Δz for cylindrical coordinate, and Δr, $r\Delta\theta$, $r\sin\theta\Delta\phi$ for spherical coordinate respectively. If these length increments are understood as the junction and/or volume lengths for the individual components, then, above equations can be written in similar finite difference forms. As shown in figure-1, one of the aims of this modification is to explore the possibility to merge the top cylinder to bottom hemi-sphere to naturally model the reactor vessel, especially lower plenum. To accomplish this aim, it is essential to identify the topological similarity between the cylindrical and spherical coordinates. As shown in equations (2.1) and (2.4), the radial directional momentum equations are similar in both coordinates, if the equivalency, $r\Delta\phi \longrightarrow r\sin\theta\Delta\phi$ and $\Delta z \longrightarrow r\Delta\theta$, is identified. This similarity can also be found in the circumferential ϕ direction in equation (2.2) and (2.5). Even though the equivalency between z and $r\Delta\theta$ is a little bit strange, if you look at the

figure-1 carefully, then, two increments are both axial increments in the respective coordinates. Therefore, one can model the downcomer and outer most region of lower plenum with a single pipe. Numbers from 1 to 18 located left-bottom of the lower sketch (vertical cross section of vessel) in fiqure-1, are volume number of a pipe. Total 18 similar pipes cover a circumference of a radial section.

Geometrical acceleration terms, signified $\overline{*}$ in the momentum transport equations, take different forms for individual coordinate. Those terms should be changed from spherical form to cylindrical form at the interface between two sections. Even though the gravitational force term in cylindrical coordinate section has only one component, z component, in spherical coordinate section, radial component of gravitational force term must be taken into account as well as the polar (θ) component. Especially, care must be exercised at the junction number 5 that connects volumes 5 and 6 in figure-1, since the vertical drop from the cylinder/sphere interface to the center of the right bellow node (volume number 5) has to be taken into account. Also, one should be careful to calculate directional cosine with enough (floating point) precision, since the minor imbalance of the gravitational terms act like pumps if any.

Even though MOD3.1 uses the central differencing scheme, modifications are made based on the upwind differencing scheme. This change is necessary to get a stable numerical scheme. In general, Bernoulli equation is not satisfied for channels with variable area in the upwind scheme. Therefore, some correction factors are to be applied. One can find that two different approaches are followed in TRACE[2] and RELAP3D[3] respectively. The best stability is found to apply, TRACE method to axial direction and RELAP3D method to radial direction respectively. There is no logical explanation to select this combination. Rather, it is determined by trial and error basis.

As one can notify in the figure-1, central part of the vessel has only three axial nodes. Some efforts has been made to make the modified code work with this kind of volume merging scheme because relatively fine noding in the downcomer and lower plenum that are necessary for analyzing those

components leads to too excessive number of node to be practical. For example, if no merging scheme were applied, number of nodes for the figure-1 case would be 5x18x18=1620, since there are 5 radial, 18 cricumferential sections, and 18 axial volumes. And, running speed is too slow to be practical even with recently purchased top level desktop personal computer. But merging the volumes in the core part into three nodes, reduce the node number to 4x18x5+18x18=684. Near 60 % reduction can be made and running speed becomes practical.

Original RELAP5/MOD3.1 has no friction for the cross flow junction. Even though the viscous terms in the above momentum equations are implemented, it is impractical to use these terms to model wall friction. The reason is that the lamina and/or turbulent viscosity are not known. Therefore, at present study, friction coefficient approach for the axial volumes in the REALP5 is extended to the cross flow junction. Correlation for axial junction is also used for the cross flow junction. But the friction for the cross flow junction is calculated using the junction velocity instead of volume velcity.

3. Description of the Input Generator

The role of Input Generator is to produce the necessary component data according to the user request. User request includes the number of sections in axial, radial and circumferential directions respectively. User also supplies the height of the cylindrical part and the radius of the spherical part. Then initial conditions for volume and junctions are to be followed. At present moment, Input Generator has built in data for generating rest of RELAP5 input deck. Friction factor is one example.

With these data, Input Generator calculates necessary items and produces RELAP5 input data for the 3D components. As shown in figure-1, the first pipe for the inner most radial section is given pipe component id 101. Then next circimferential pipe is given 102, and so on. Last pipe id for this section is 118. Next 18 numbers from 119 to 136 is given to circumferential multiple junctions that connect neighboring pipes from 101 through 118 and again to 101. Next 18 numbers from 137 to 154 are given to

radial multiple junctions that connect pipes in first radial section to the pipes in the second radial section whose pipe id starts form 201, ends 218. This assignment scheme continues to the last radial section, radial section number 5 for this problem. Therefore, pipe id 501 is the first pipe in the outer most radial section. If any merging scheme is requested, then pipe axial node number is adjusted accordingly. And the generator sets the number of axial volume for the specific radial section to appropriate number so that 3D module calculates the momentum flux and other parameters up to the set volume. For the figure-1, from radial section 1 to radial section 4, 3D module calculates only up to node 5. These RELAP5 component data are written to the input file, INDTA, by calling subroutines, such as, generator_pipe, generator_mtpljun_ circular, and generator_mtpljun_radial in turn (figure-2).

Next, connectivity data are generated in the subroutine generator_connection (figure-2) that is used in the RELAP5 subroutine TRNSET to tag the volumes and junctions that are involved in 3D business. Input Generator finishes its work by producing the relevant boundary conditions. The structure of the Input Generator is shown in Figure-2.

4. Test Run

Even though multi-dimensional computer codes, such as RELAP5-3D, TRAC[5], COBRA-TF[4], and TRACE , have been introduced quite a long time, as far as I know, any real problems that are indispensable with those codes are not found. But, DVI design adopted in APR-1400 raises a significant questions concerning the applicability of the one dimensional computer code because of its very nature of multi-dimensional behavior in the downcomer. Therefore, the first test case is the simplified vessel model with DVI. The schematic diagram of the model is shown in figure-1. It is a vessel with DVI, which is initially filled up to volume-13, cold leg level. Then, steam from the intact cold legs, C1,C2,and C3, blows. Safety injection from the SI nozzles S1 and S2, located at volume-16 in pipe-7 and 16, starts at the beginning. The aim of this run is to see the flow behavior in the downcomer and lower plenum.

The best parameter, to check whether the calculation can reach the stable condition or not, is to show the temporal behavior of the downcomer collapsed level. 2D surface plot or contour plot of the level shows rather clear vision of it. The downcomer collapsed water level which is initially 5.2m reduced to about 3m due to the blowing steam as shown in figure-3. Passing the transient time of 400 seconds, it maintains the level through the rest of time. Figure-3 shows a deep valley at around pipe number 10. This valley can also be found in contour map figure-4. To find the reason of the developed valley, it is necessary to look at the velocity profile, condensation rate distribution, and void fraction altogether.

In figure-5, vector plot of the vapor velocity shows several interesting points. Steam that comes in from 3 (red) intact cold legs blows toward the broken cold leg. But, it feels the existence of the (black) hot legs that are not to be penetrated. Sudden reduction in velocity just in front of the hot legs tells this. Steam flows downward or upward to pass the hot legs. Steam flow near the C_3 meets the injected cold lquid flow. Therefore, it leans more upward compared to the flow near C_1, which is rather far from SI. This leaning effect is also related with the condensation rate. Strong suction from the broken cold leg B shows the acceleration near it. The velocity distribution in the upper downcomer partly tells us that the two dimensional calculation is reasonably performed in the developed 3D module.

Liquid velocity distribution in downcomer is shown in figure-6. Overall distribution of liquid velocity is also reasonable. Especially, liquid velocity near S_2 tells that injected liquid with the condensate suspends in the top region by steam blow from two cold legs, C_2 and C_3. The presence of hot leg, H_2, helps this suspension. Anyway, this suspended liquid flows toward broken cold leg almost horizontally, but it drops to the lower downcomer without reaching the broken cold leg. This can be confirmed by the velocity vector, marked by * right below B. It misses hitting B by shifting right. But, velocity vectors at pipe number 9 near B direct downward. Altogether, liquid flow from the right hand side can not reach the broken cold leg. Instead, it falls to the lower plenum.

Figure-7 shows the distribution of the condensation in the downcomer. The momentum, imparted

by liquid flow from S_2 with the condensate produced nearby, pushes the water level downward. This push down effect is well shown in figure-8. Liquid fraction contour in downcomer shows the dip at pipe 10 node 8 and 9. Total mass flow in figure-8, also shows very well the liquid flow pattern at upper downcomer. As mentioned above, relatively high liquid fraction at top right corner comes from the blown SI flow and the condensate. It directs downward at pipe 12, and reaches water surface at middle of pipe-10 and 11. Injected flow from S1, which is very near the broken leg, is sucked out by brow-out steam at B.

Total mass flow depicted at figure-8 shows the interesting flow pattern at the liquid filled region in the lower downcomer. It clearly shows a pattern. The main circulation happens due to the push-effect mentioned above. The large mass flow rate at pipe-10 from node-5 to node-9 drives the circulation. The driving force maintains the circulation even in the lower plenum region that covers the area below node-5. At this point, one can understand the various and consistent reasons of the existence of the deep valley located at pipe-10 in figure-3. It seems to be another relatively strong downward push below C_1 because average collapsed water level is maintained low (figure-3) and low liquid fraction (figure-9).

5. Conclusions and further study

Overall behavior in the vessel depicted at various figures tells us that the developed 3D module works fine. Remembering that all kinds of unstable behavior experienced during the development, I am happy to have the tidy results shown in section 4. Of course, many aspects that are to draw further study are identified during the development. For example, models and correlations should be reexamined to check their appropriateness. Running speed optimization, user-friendly code, extending Input Generator, efficient output procedure are tasks for the near future. Some more aggressive trial applications are corner stone to get a perspective view of future.
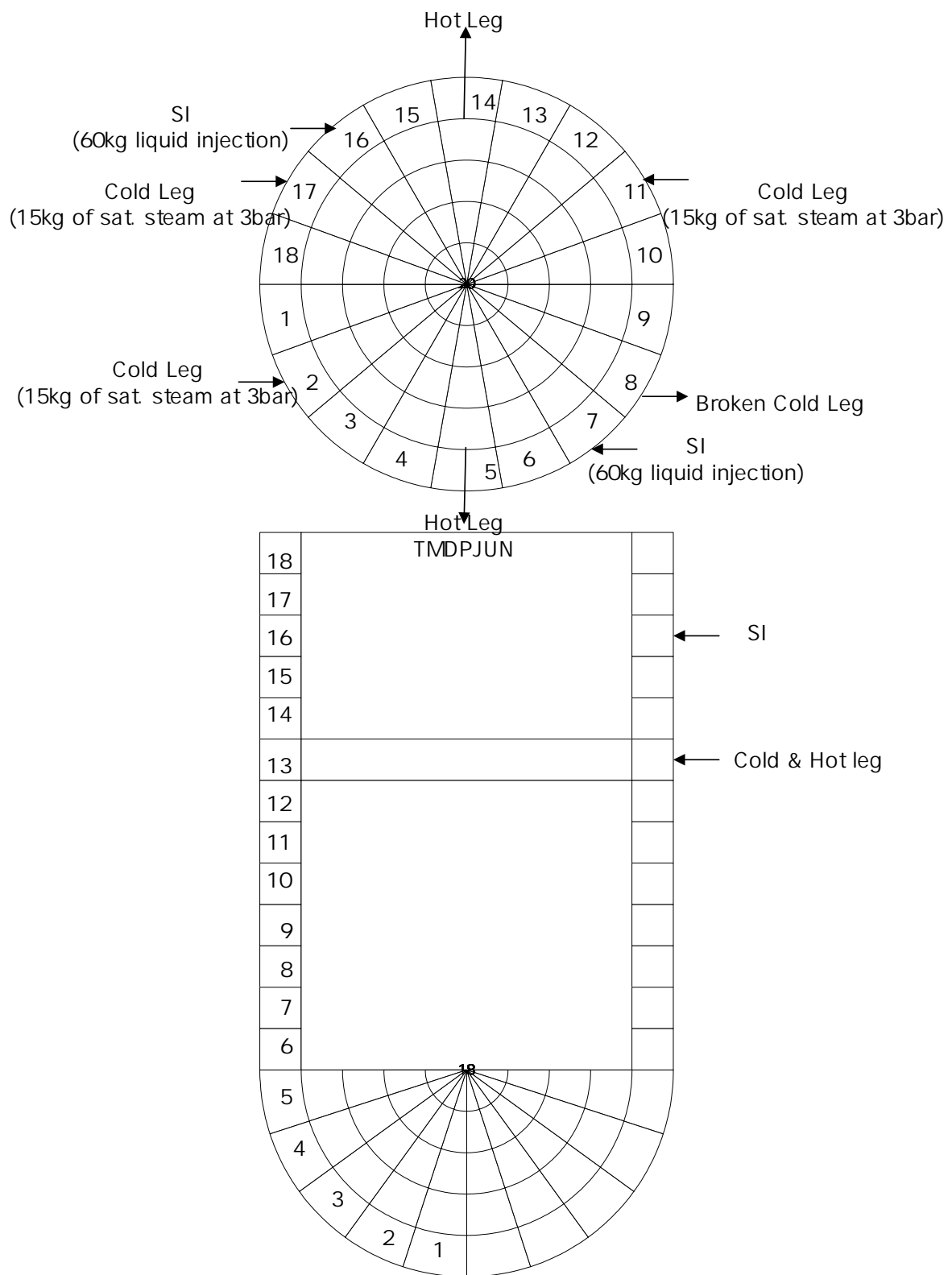
Figure-1 Vessel Nodalization for test Case

```
program multid_input_generator
        use geometry_3d_module
        define problem constants
        allocate variables for geometry_3d_module
        call generator
        call generator_output
                call generator_pipe
                call generator_mtpljun_circular
                call generator_mtpljun_radial
                call generator_connection
                call generator_boundary_condition_core
                call generator_boundary_condition_coldleg
                call generator_boundary_condition_hotleg
                call generator_boundary_condition_dvi
        end subroutine generator_output
end problem multid_input_generator
```

Figure-2. Structure of Input Generator

Downcomer Collapsed Water Level
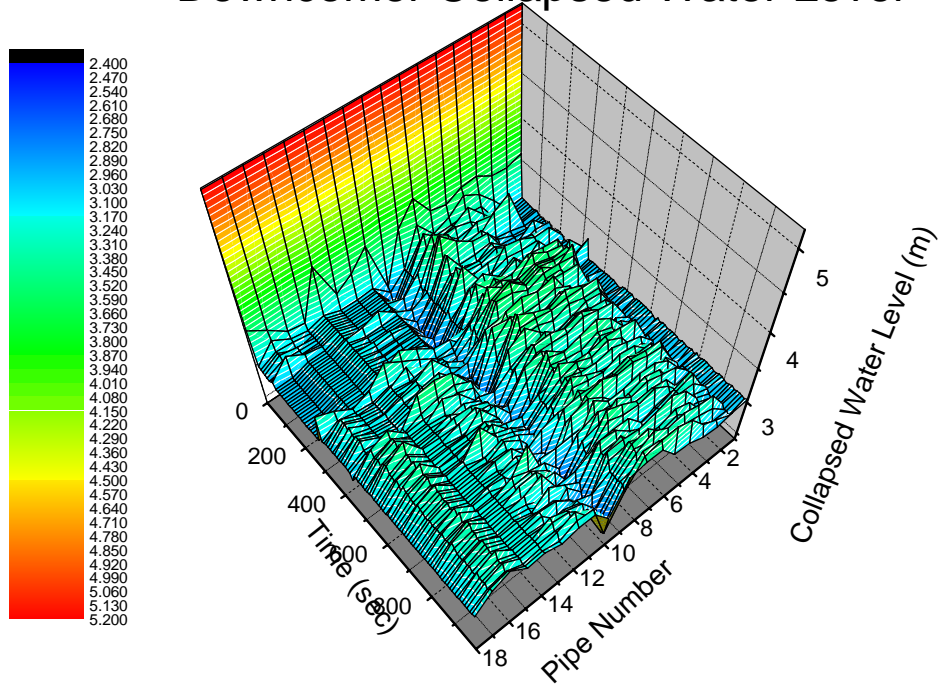
Figure-3. Downcomer Collapsed Water Level
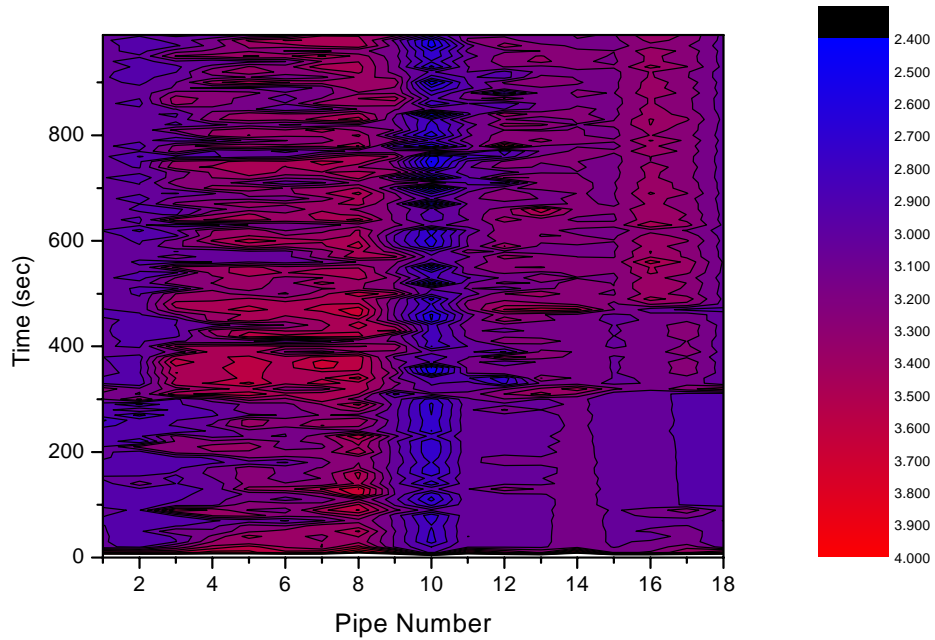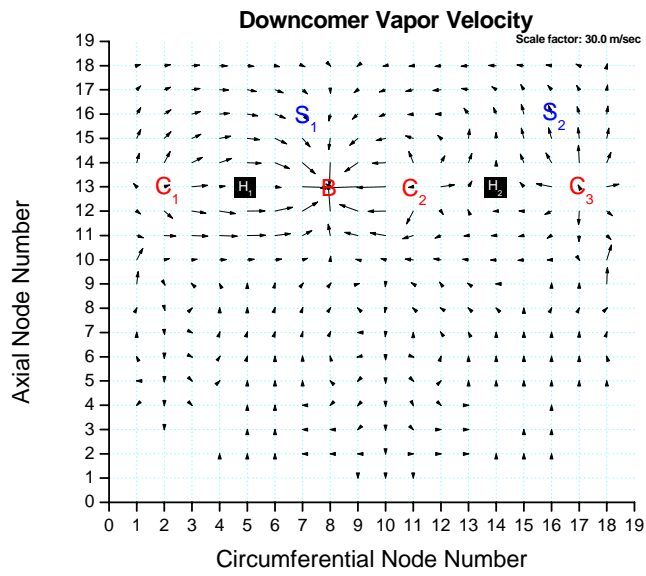

Figure-4. Downcomer Collapsed Water Level Contour Map

Downcomer Vapor Velocity

Figure-5. Downcomer Vapor Velocity (550 sec)
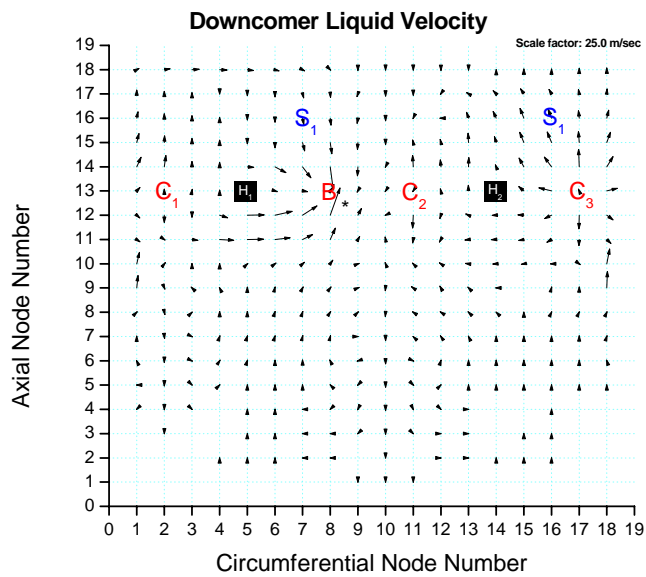
Downcomer Liquid Velocity
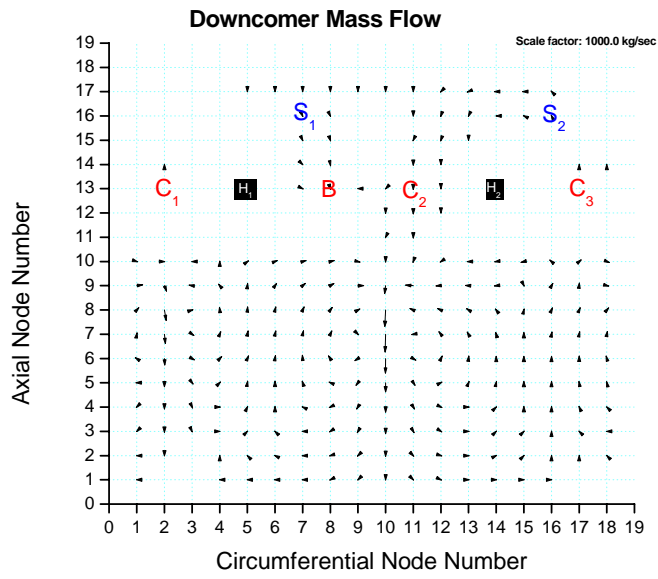
Figure-6. Downcomer Liquidr Velocity (550 sec)
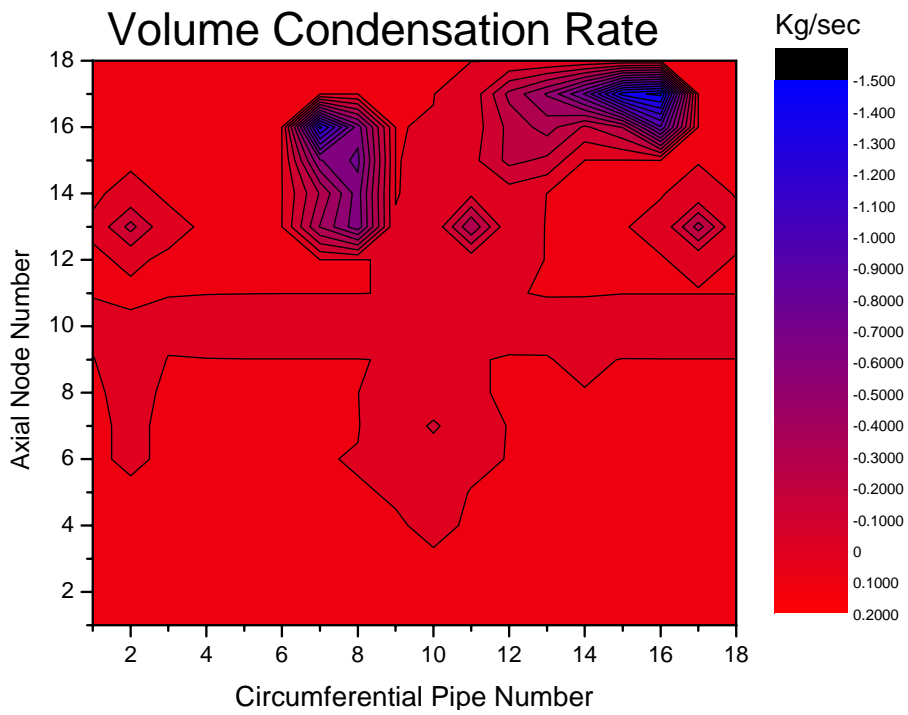
Figure-7. Downcomer Total Mass Flow Rate (550 sec)
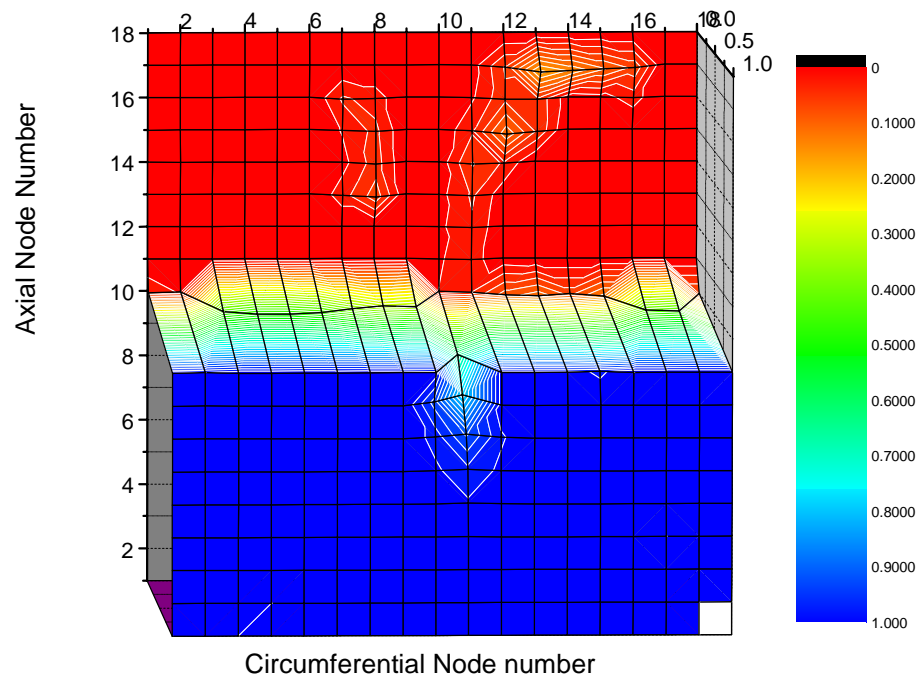

Figure-8. Volume Condensation Rate (550 sec)

Figure-9. Downcomer Void Fraction Contour (550 sec)

REFERENCES

1. K. Carlson, et al., "RELAP5/MOD3 Code Manual," EG&G Idaho, Inc., NUREG/CR-5535, June 1990.

2. J. W. Spore, et al., (TRACE) "TRAC-M/FORTRAN 90 (VERSION 3.0), THEORY MANUAL", LA-UR-00-910, Los Alamos National Laboratory , Los Alamos, New Mexico , July 2000.

3. RELAP5-3D The RELAP5-3D Code Development Team, RELAP5 code manual volume IV-Models and Correlation, INEEL-EXT-98-00834 Rev.02, INEEL, July 2002.

4. PNL, "COBRA/TRAC – A Thermal-Hydraulics Code for Transient Analysis of Nuclear Reactor Vessels and Primary Coolant Systems," NUREG/CR-3046, March 1983.

5. LANL, "TRAC-PF1/MOD1: An Advanced Best-Estimate Computer Program for Pressurized Water Reactor Thermal-Hydraulic ANALYSIS," NUREG/CR-3858, July 1986.